Advances in Biomechanics and Applications, *Vol. 1, No. 2 (2014) 95-109*
DOI: http://dx.doi.org/10.12989/aba.2014.1.2.095

Simulation of tissue differentiation around acetabular cups: the effects of implant-bone relative displacement and polar gap

Kaushik Mukherjee[a] and Sanjay Gupta[*]

Department of Mechanical Engineering, Indian Institute of Technology Kharagpur, Kharagpur 721302, West Bengal, India

(Received October 10, 2013, Revised January 9, 2014, Accepted January 24, 2014)

Abstract. Peri-acetabular bone ingrowth plays a crucial role in long-term stability of press-fit acetabular cups. A poor bone ingrowth often results in increased cup migration, leading to aseptic loosening of the implant. The rate of peri-prosthetic bone formation is also affected by the polar gap that may be introduced during implantation. Applying a mechano-regulatory tissue differentiation algorithm on a two-dimensional plane strain microscale model, representing implant-bone interface, the objectives of the study are to gain an insight into the process of peri-prosthetic tissue differentiation and to investigate its relationship with implant-bone relative displacement and size of the polar gap. Implant-bone relative displacement was found to have a considerable influence on bone healing and peri-acetabular bone ingrowth. An increase in implant-bone relative displacement from 20 μm to 100 μm resulted in an increase in fibrous tissue formation from 22% to 60% and reduction in bone formation from 70% to 38% within the polar gap. The increase in fibrous tissue formation and subsequent decrease in bone formation leads to weakening of the implant-bone interface strength. In comparison, the effect of polar gap on bone healing and peri-acetabular bone ingrowth was less pronounced. Polar gap up to 5 mm was found to be progressively filled with bone under favourable implant-bone relative displacements of 20 μm along tangential and 20 μm along normal directions. However, the average Young's modulus of the newly formed tissue layer reduced from 2200 MPa to 1200 MPa with an increase in polar gap from 0.5 mm to 5 mm, suggesting the formation of a low strength tissue for increased polar gap. Based on this study, it may be concluded that a polar gap less than 0.5 mm seems favourable for an increase in strength of the implant-bone interface.

Keywords: tissue differentiation; bone ingrowth; acetabular polar gap; bone healing; finite element analysis

1. Introduction

Over the last few decades, uncemented porous coated acetabular components have been a preferred alternative to cemented fixation (National Joint Registry 2012, New Zealand Joint Registry 2012, Norwegian Arthroplasty Register 2010, Slovakian Arthroplasty Register 2011) since it offered better long-term fixation with bone. Cast-in Cobalt Chrome (CoCr) beaded surface having Hydroxyapatite (HA) coating on ADEPT and Birmingham Hip Resurfacing (BHR) cups

∗Corresponding author, Associate Professor, E-mail: sangupta@mech.iitkgp.ernet.in
[a]Ph.D. Student, E-mail: kaushik.mukherjee@mech.iitkgp.ernet.in

http://www.techno-press.org/?journal=aba&subpage=7 ISSN: 2287-2094 (Print), 2287-2272 (Online)

has demonstrated high clinical success (Daniel *et al.* 2004, Itayem *et al.* 2005, Back *et al.* 2005, Treacy *et al.* 2005, Treacy *et al.* 2011). The immediate post-operative stability of these uncemented implants is attained by press-fit fixation by inserting an oversized acetabular cup into an under-reamed acetabulum. After initial deformation due to impaction, the surrounding bone, by virtue of its elastic and viscoelastic properties, partially returns to its undeformed shape. Consequently, a compressive force is being applied on the acetabular cup surface leading to a stable initial post-operative fixation (Curtis *et al.* 1992).

Although press-fit fixation of acetabular cup increases the peripheral contact between the cup and the bone, leading to bone ingrowth (Peters and Miller 2006), this may also lead to the incidence of acetabular polar gap in some cases due to insufficient impaction. The polar gap is often found to increase with larger press-fit acetabular cup (MacKenzie *et al.* 1994). Bone mineralization is also found to increase for a gap of 0.5 mm or less (Sandborn *et al.* 1988). However, most of the clinical studies have reported substantial bone ingrowth within this gap, which suggest that the initial polar gap may have minimal influence on the clinical outcome of uncemented acetabular replacements (Schmalzried *et al.* 1994, Udomkiat *et al.* 2002, Springer *et al.* 2008, Takao *et al.* 2011, Nakasone *et al.* 2012).

Bone ingrowth is a complex biological phenomenon that follows the similar process of primary bone fracture healing (Davies 1996, 2003) and is known to depend on implant-bone relative displacement. A well-controlled and adequate mechanical loading with low implant-bone relative displacement (~20 μm) leads to bone ingrowth in the implant-bone interface (Prendergast *et al.* 1997, Hollister *et al.* 1996, Puleo *et al.* 1999, Liu and Niebur 2008). In comparison, a high implant-bone relative displacement in the range of ~100 μm and 150 μm led to the formation of cartilage and fibrous tissue (Haddad *et al.* 1987, Jasty *et al.* 1991, 1997, Engh *et al.* 1987, Bragdon *et al.* 2004). The generation of fibrous tissue, instead of bone, leads to weakening of the implant-bone interface strength (Haddad *et al.* 1987, Jasty *et al.* 1991, 1997) and thereby, causes implant loosening in long-term (Engh *et al.* 1987, Bragdon *et al.* 2004).

In order to describe the mechano-regulatory tissue differentiation, several algorithms have been developed which were broadly based on two approaches: one employing linear elastic material property to model the tissue (Carter *et al.* 1988, Claes and Heigele 1999), and the other implementing biphasic poroelastic material model to simulate the coupled fluid and solid phase of the tissue (Huiskes *et al.* 1997, Prendergast *et al.* 1997, Lacroix and Prendergast 2002, Lacroix *et al.* 2002). Both the approaches led to consistent predictions of tissue differentiation in bone fracture healing (Isaksson *et al.* 2006). Such algorithms were also used for design evaluations of glenoid components (Andreykiv *et al.* 2008), short stemmed metaphyseal loading implant (Puthumanapully and Browne 2011), multi-layered Porocoat® Beaded Coating (Puthumanapully 2010) and dental implants (Chou and Müftü 2013). These algorithms were also combined with bone remodelling to predict the bone adaptation around porous coated implant (Liu and Niebur 2008) and resurfacing femoral implant (Dickinson *et al.* 2012). However, none of these studies considered the presence of implant-bone gap in the microscale beaded model and investigated the influence of this gap on the bone ingrowth pattern to determine the critical implant-bone gap.

Bone healing within the acetabular polar gap may alter the distribution of mechanical loading and, thereby, influence bone remodelling around the acetabular component. However, there is scarcity of numerical study to predict peri-acetabular bone ingrowth and its relationship with acetabular polar gap. Consequently, most of the three-dimensional (3-D) numerical studies of bone adaptation around the acetabular component modelled the implant-bone interface as either bonded (Manley *et al.* 2006, Ghosh *et al.* 2013) or debonded (Ghosh *et al.* 2013), which might not be

entirely representative of the physiological condition. Therefore, development of a numerical model to investigate peri-prosthetic bone formation and its relationship with polar gap and implant-bone relative displacement might lead to more realistic evaluation of the peri-acetabular interface. Acetabular polar gap and implant-bone relative displacement are hypothesized to affect the tissue differentiation across the gap and, thereby, influence the long-term fixation of the implant with bone. Applying a mechano-regulatory tissue differentiation algorithm on a 2-D plane strain microscale model, representing implant-bone interface, the objectives of the present study are to gain an insight into the process of peri-prosthetic tissue differentiation and to investigate its relationship with implant-bone relative displacement and size of the polar gap.

2. Materials and methods

2.1 Development of 2D cast-in beaded implant model

A 2-D microscale solid model of implant-bone interface, consisting of cast-in beaded implant, granulation tissue and bone, was developed using SolidWorks software (Dassault SolidWorks Corp., Concord, MA, USA). The bead diameter was calculated by fitting a circle through the cross-section of the BHR acetabular cup (Morrison 2006), using least square method (Figs. 1(a)-(d)). The thickness of the beaded layer was assumed to be 931 μm (FDA 2006). Average porosity was assumed to be 34% for the beaded layer (FDA 2006). Bead diameter was found to be 1100 µm. The model represented a cross section through a 3-D structure of the implant-bone interface. In order to simulate the effect of implant-bone relative displacement on bone healing around uncemented cast-in beaded implant, a polar gap of 0.5 mm, initially filled with granulation tissue, was assumed to be present between the bone and implant-bead (Fig. 1(e)). Additionally, the effect of the presence of polar gap between bone and implant on bone healing and peri-acetabular bone ingrowth was investigated using five models with different polar gaps of 0.5 mm, 1 mm, 1.5 mm, 2 mm and 5 mm.

The 2-D solid models were meshed using plane strain eight noded quadrilateral element, with maximum edge length of 20 µm, using ANSYS FE software (ANSYS Inc., Canonsburg, PA, USA). The number of nodes and elements corresponding to different FE models are presented in the Table 1. Linear, elastic, homogeneous and isotropic material property was assumed for all materials. Young's modulus of 500 MPa was assigned to bone tissue (Puthumanapully 2010) whereas, the Young's modulus of implant as well as beads was assumed to be 210 GPa. Poisson's ratios for both the bone tissue and implant were assumed to be 0.3. The interfaces between implant bead and granulation tissue and granulation tissue and bone were assumed to be bonded.

2.2 Applied boundary condition

In order to analyse the effect of implant-bone relative displacement on bone healing and peri-prosthetic bone ingrowth, the 2-D model with 500 µm gap between implant and bone, was considered. Three different levels of tangential displacement boundary conditions, 20 μm, 60 μm and 100 μm, were prescribed at the bottom of the implant along the positive *x*-direction (Fig. 1(e)). Additionally, a normal displacement of 20 μm in the positive y-direction was also applied at the bottom of the implant to simulate the movement of the acetabular cup due to hip joint reaction force (Fig. 1(e)). The top boundary of bone was fully constrained in all directions. Periodic

boundary conditions were prescribed on both the lateral surfaces to represent the repeating unit of the model in the macroscopic implant-bone interface.

In the second part of the study, the effect of polar gap on bone healing and peri-prosthetic bone ingrowth was investigated. Displacements of 20 μm along normal and 20 μm along tangential directions were prescribed at the bottom of the implant for all the FE models, having different polar gaps. All other boundary conditions were similar to the earlier case (Fig. 1(e)).

Table 1 Number of elements and nodes in each region of different finite element models

FE Model Parts / FE Model Specifications	Bone		Tissue		Beaded Implant	
	Number of Elements	Number of Nodes	Number of Elements	Number of Nodes	Number of Elements	Number of Nodes
Model 1: 500 μm gap	17500	53301	13875	42780	31667	96280
Model 2: 1000 μm gap	17500	53301	22706	69235	31667	96280
Model 3: 1500 μm gap	17500	53301	31039	94262	31667	96280
Model 4: 2000 μm gap	17500	53301	40588	122973	31667	96280

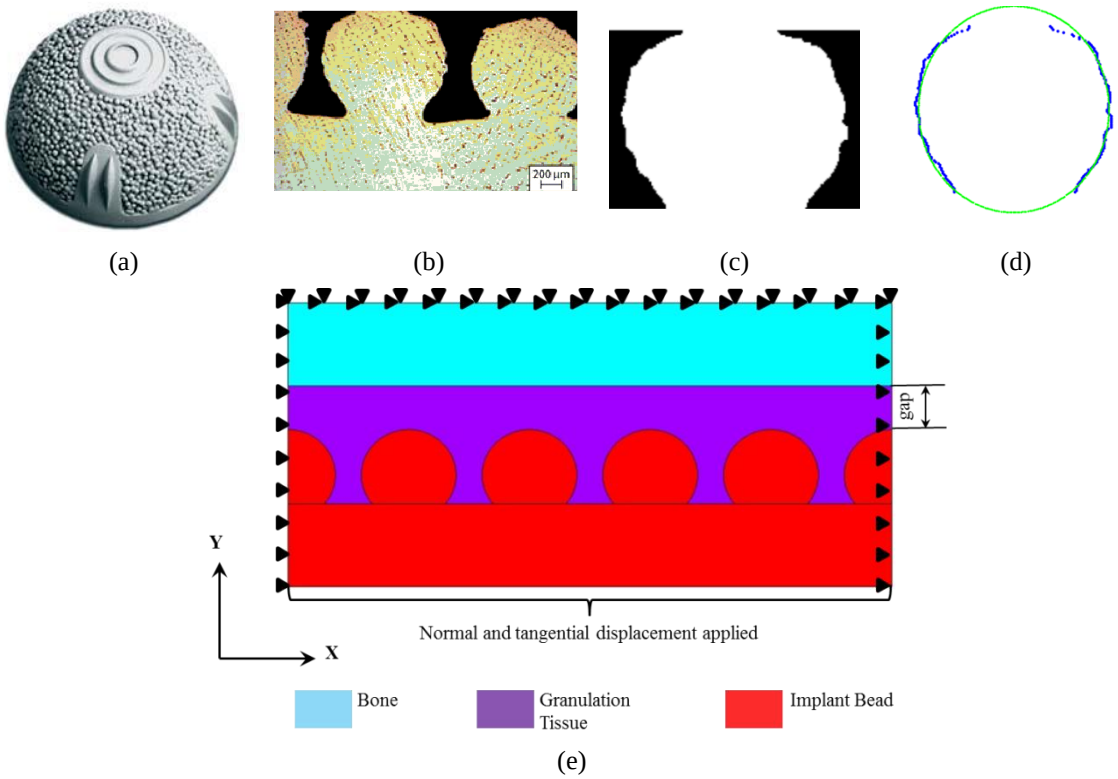

Fig. 1 Development of 2-D microscale plane strain model of implant-bone interface: (a) BHR acetabular cup (adopted from Morrison 2006); (b) Cross-section of the Porocast bead (adopted from Morrison 2006); (c) 2nd bead, from left, as read by Matlab; (d) Circle fitted through the points of the 2nd bead following Least Square Error Principle; e) The solid 2-D plane strain model showing granulation tissue occupying the gap in between the bone and Porocast bead

Table 2 Material properties applied to the tissues and associated stimulus levels. (Claes and Heigele 1999, Isaksson *et al.* 2006, Dickinson *et al.* 2012)

Tissue phenotype	Young's modulus	Poisson's Ratio	Strain stimulus (%)	Hydrostatic pressure stimulus (MPa)
Granulation tissue	1	0.167	–	–
Fibrous tissue	2	0.167	–	>0.15
			>5	>–0.15
			<–5	>–0.15
Cartilage	10	0.167	>15	<–0.15
			<–15	<–0.15
Immature bone	1000	0.3	–15 to +15	<–0.15
Mature bone	6000	0.3	–5 to +5	–0.15 to +0.15

2.3 Tissue differentiation algorithm

Implant-bone interface adaptation is known to follow a sequential, mechano-regulatory tissue differentiation algorithm, wherein depending upon the local mechanical stimulus, the migrated mesenchymal stem cells (MSC) differentiate into different connective tissue phenotypes (Liu and Niebur 2008, Dickinson *et al.* 2012, Chou and Müftü 2013). In this study, initially the polar gap was assumed to be filled with granulation tissue. The migration and proliferation of MSC within the granulation tissue was modelled by using the principle of diffusion as stated in the following Eq. (1) (Lacroix and Prendergast 2002)

$$\frac{\mathbf{d}\rho}{\mathbf{dt}} = \mathbf{k}\nabla^2\rho \tag{1}$$

where, ρ is the local cell concentration and k is the diffusion constant. The value of k was chosen such that the process of MSC migration and proliferation will be completed within 16 weeks (Lacroix and Prendergast 2002). The bone boundary, adjacent to the granulation tissue layer, was assumed to be rich in MSC concentration and was assumed to act as an MSC source for this diffusion process. A zero diffusion boundary condition was imposed on all the other boundaries of the granulation tissue layer, representing no cell loss from the granulation tissue during the diffusion process.

In order to model the differentiation and maturation of MSCs, the following mechano-regulatory principle was employed (Lacroix and Prendergast 2002). Depending on the local mechanical stimuli, comprising of hydrostatic pressure and deviatoric strain (Table 2), the MSC would differentiate into different target phenotypes (fibroblast, chondrocyte or osteoblast) (Claes and Heigele 1999). These target phenotypes upon maturation would be transformed into different connective tissues (fibrous tissue, cartilage or bone) (Claes and Heigele 1999). The temporal evolution of mechano-regulated tissue phenotypes would lead to the simultaneous presence of granulation tissue as well as differentiated tissue at any instantaneous time. Therefore, a rule of mixture, using Eq. (2), was implemented to calculate the element elastic properties, such as Young's modulus and Poisson's ratio

$$\mathbf{E}_{\mathbf{n}+1} = \left(\frac{\rho_{max} - \rho}{\rho_{max}}\right)\Bigg|_{\mathbf{n}} \mathbf{E}_{\mathbf{granulation}} + \left(\frac{\rho}{\rho_{max}}\right)\Bigg|_{\mathbf{n}} \mathbf{E}_{\mathbf{tissue}} \tag{2}$$

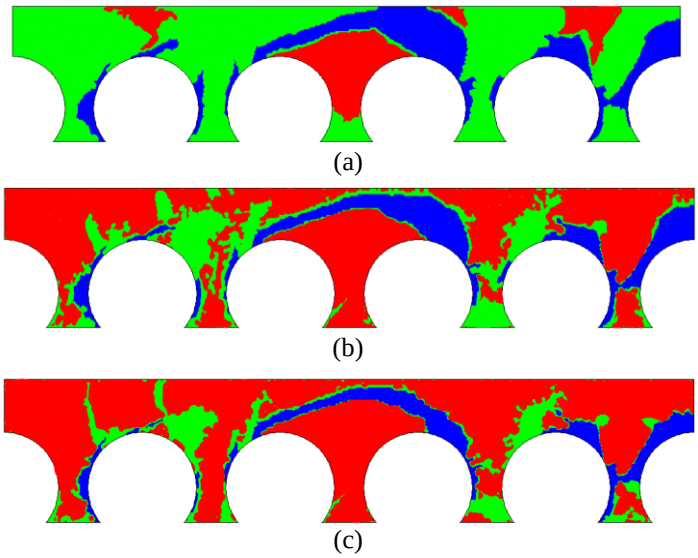

Fig. 2 Predicted tissue differentiation pattern corresponding to iterations for 20 μm normal and 20 μm tangential displacement, with a polar gap of 0.5 mm: (a) after 30 iterations; (b) after 180 iterations; (c) after attainment of equilibrium (Red: Bone; Green: Cartilage; Blue: Fibrous Tissue)

where, E_{n+1} is the local elastic properties of a single element at the end of n-th iteration; ρ is the concentration of cells in the element after n-th iteration and ρ_{max} denotes the maximum cell concentration in an element; $E_{granulation}$ and E_{tissue} are the elastic properties of the granulation tissue and differentiated tissues, respectively, which are given in Table 2 (Isaksson *et al.* 2006, Dickinson *et al.* 2012, Liu and Neibur 2008). In order to avoid numerical instabilities due to sudden change in tissue phenotypes between any two consecutive iterations, a temporal smoothing technique was implemented by averaging the local elastic properties over ten previously calculated values of elastic properties (Lacroix and Prendergast 2000), given below in Eq. (3)

$$\mathbf{E_{n+1,smoothed}} = \frac{1}{10}\sum_{\mathbf{i=n}}^{\mathbf{n-9}} \mathbf{E_i} \tag{3}$$

A Matlab script (Matlab 2013a, The MathWorks Inc., Natick, MA, USA) was developed to implement the tissue differentiation algorithm. Another separate master batch script was created to sequentially launch ANSYS Software for FE analysis and Matlab for tissue differentiation calculations, for each iteration. The whole simulation was run in batch mode in a Windows 2012 server with two Intel Xeon 12-core CPUs and 64 GB RAM. In this simulation, a single iteration was assumed to represent one day. This iterative simulation was set to run for a specified number of 730 iterations (365 days×2), representing a two-year post-operative period. Convergence in tissue formation was assumed to be attained when the change in tissue phenotype in an element was less than 1% between two successive iterations.

2.4 Mesh convergence study

The accuracy of the FE predicted results was checked using a mesh convergence study based on von

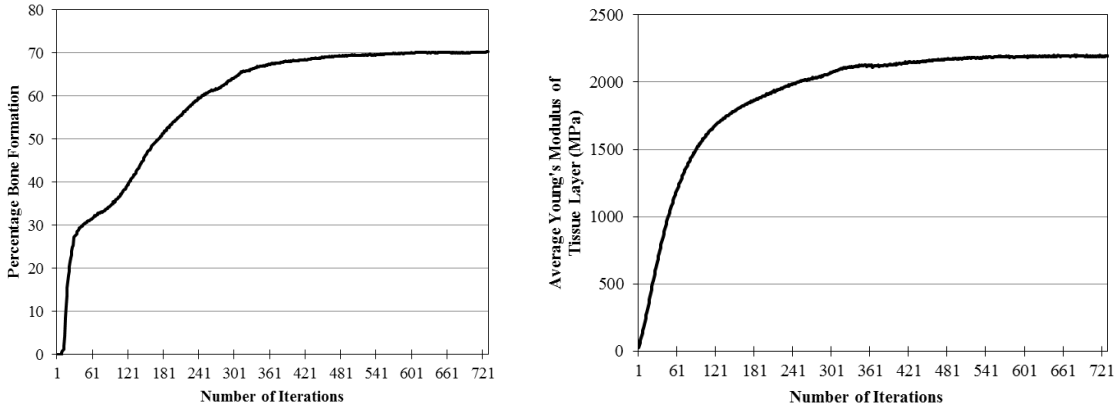

(a) (b)

Fig. 3 Variation of tissue phenotype and tissue Young's modulus with number of iterations: (a) Percentage of bone formed within the gap; (b) Average Young's modulus of the tissue layer

Mises stress generated within the granulation tissue. Three 2-D FE models of beaded interface, with 500 μm polar gap, were developed with elements of edge length 40 μm, 20 μm and 10 μm resulting into 15665, 63042 and 246183 number of elements in the respective FE models. The normal (20 μm) and tangential (20 μm) displacements were prescribed at the bottom of the implant, while fully constrained and periodic boundary conditions were applied on the top bone-boundary and lateral surfaces, respectively. Deviations in the von Mises stress ranging between 12% - 15% were observed between the first and second models, whereas, these deviations were reduced to 1% - 2% between the second and third models. The third FE model with 246183 elements being computationally expensive, the second FE model having 63042 elements and maximum edge length of 20 μm was chosen for further analysis.

3. Results

The peri-acetabular tissue growth simulation for the model having 0.5 mm polar gap with 20 μm normal and 20 μm tangential displacements clearly showed the gradual temporal transformation of initial granulation tissue into bone, cartilage and fibrous tissue (Figs. 2(a)-2(c)). Initially, a large amount of cartilage (~55%-70%) was formed in the gap. However, a major portion of the cartilage was transformed to bone, progressively, leading to predominant bone formation in the polar gap, amounting to ~70% of the gap (Figs. 2(a)-(c), 3(a)). Consequently, the average Young's modulus of the tissue layer gradually increased upto ~2200 MPa (Fig. 3(b)). Moreover, high bone ingrowth was observed, progressively, at the implant boundary within the inter-bead spacing, which suggested an improved fixation of implant with bone.

3.1 Effect of implant-bone relative displacement

Implant-bone relative displacement was found to affect the extent of tissue growth in the polar gap. For moderate tangential displacement of 60 μm, the model indicated considerably less bone formation (~47%), as compared to the model with lower tangential displacement of 20 μm (Figs.

4(a)-(b), 5(a)). Moreover, the amount of cartilage formation was also reduced to ~4%. Fibrous tissue formation was predominantly high, occupying ~50% of polar gap. The average Young's modulus of the tissue layer was considerably reduced from ~2200 MPa to ~1500 MPa (Fig. 5(b)).

This newly formed layer of fibrous tissue separated the bone layers adjacent to the implant-bead and the top bone-boundary (Fig. 4(b)).

In the case of tangential displacement of 100 µm, results indicated further reduction in bone (~38%) and cartilage formation (~2%) (Figs. 4(c), 5(a)). For this condition, fibrous tissue was formed in major portion (~60%) of the polar gap (Figs. 4(c), 5(a)), leading to comparatively low average Young's modulus (~1200 MPa) of the tissue layer (Fig. 5(b)). Although reduced peri-prosthetic bone formation was observed, they were quite localised in nature (Fig. 4(c)). Therefore, an increase in implant-bone relative displacement resulted in the weakening of implant-bone interface strength.

3.2 Effect of acetabular polar gap

Variation in polar gap was found to be less pronounced on the extent of tissue formation in the gap. Application of 20 µm normal and 20 µm tangential displacements resulted in predominant bone formation near the top boundary as well as within inter-bead space (Figs. 6(a) – (e), (a)). With an increase in polar gap, the formations of fibrous tissue and cartilage around the implant beads were reduced. During early post-operative stage, however, the cartilage formation was increased from 50% to 90% of polar gap for an increase in gap from 0.5 mm to 5 mm. Consequently, the initial rate of bone formation was reduced for an increase in polar gap (Fig. 7(a)). However, the overall percentage bone formation after attainment of equilibrium increased from ~70% to ~94% for an increase polar gap from 0.5 mm to 5 mm (Fig. 7(a)). In spite of predominantly high bone formation in the polar gap, the average Young's modulus of the tissue

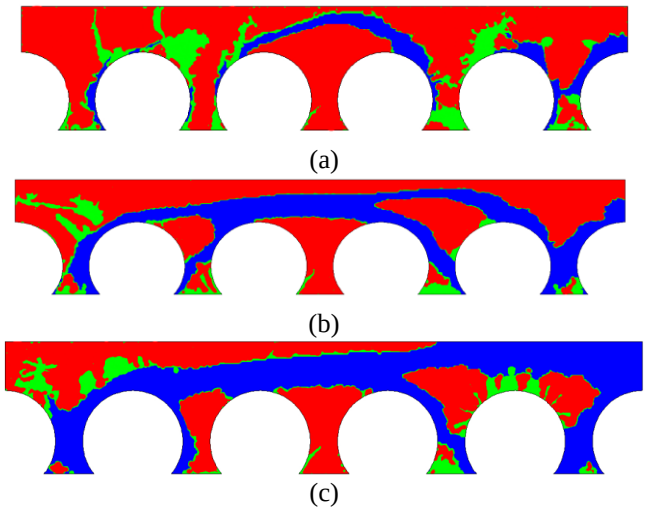

Fig. 4 Predicted tissue differentiation pattern after attainment of equilibrium for different implant-bone relative displacements, with a polar gap of 0.5 mm: (a) 20 μm normal, 20 μm tangential displacement; (b) 20 μm normal, 60 μm tangential displacement; (c) 20 μm normal, 100 μm tangential displacement (Red: Bone; Green: Cartilage; Blue: Fibrous Tissue)

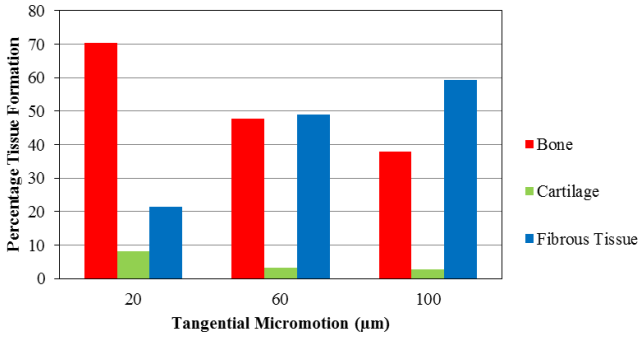

(a)

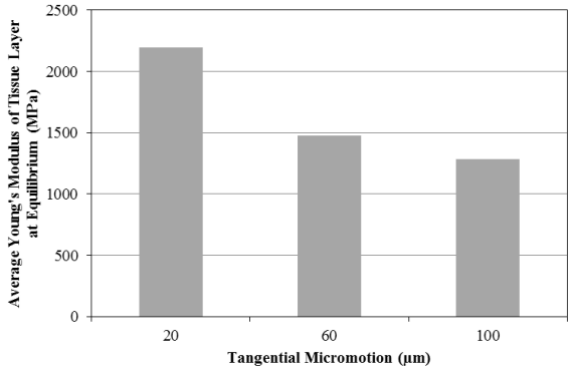

(b)

Fig. 5 Variation of major tissue phenotypes and tissue Young's modulus after attainment of equilibrium for different tangential relative displacements: (a) Percentage of bone, cartilage and fibrous tissue formed within the gap; (b) Average Young's modulus of the tissue layer

layer was found to decrease for an increase in the polar gap (Fig. 7(b)). These results suggest that an increase in polar gap enhances the formation of immature bone, and thereby, results in the formation of a low strength tissue within the gap.

4. Discussions

Peri-acetabular bone ingrowth plays a crucial role in enhancing the long-term stability of press-fit acetabular cups. A poor bone ingrowth often results in increased cup migration leading to aseptic loosening of the cup. Polar gap, if present, is also found to affect the rate of peri-prosthetic bone growth, although they might disappear with time due to proper bone healing within the gap. Despite few clinical studies on bone healing in the polar gap (Sandborn *et al.* 1988, Schmalzried *et al.* 1994, Udomkiat *et al.* 2002, Springer *et al.* 2008, Takao *et al.* 2011, Nakasone *et al.* 2012), to the authors' knowledge, there is scarcity of numerical analysis to predict the bone healing and its relationship with polar gap. In this present study, a mechano-regulatory tissue differentiation algorithm is applied to a microscale 2-D FE model of cast-in BHR beads and bone interface, with varying polar gap, in order to investigate the effects of implant-bone relative displacement and the gap size on the extent bone healing in polar gap and peri-prosthetic bone ingrowth.

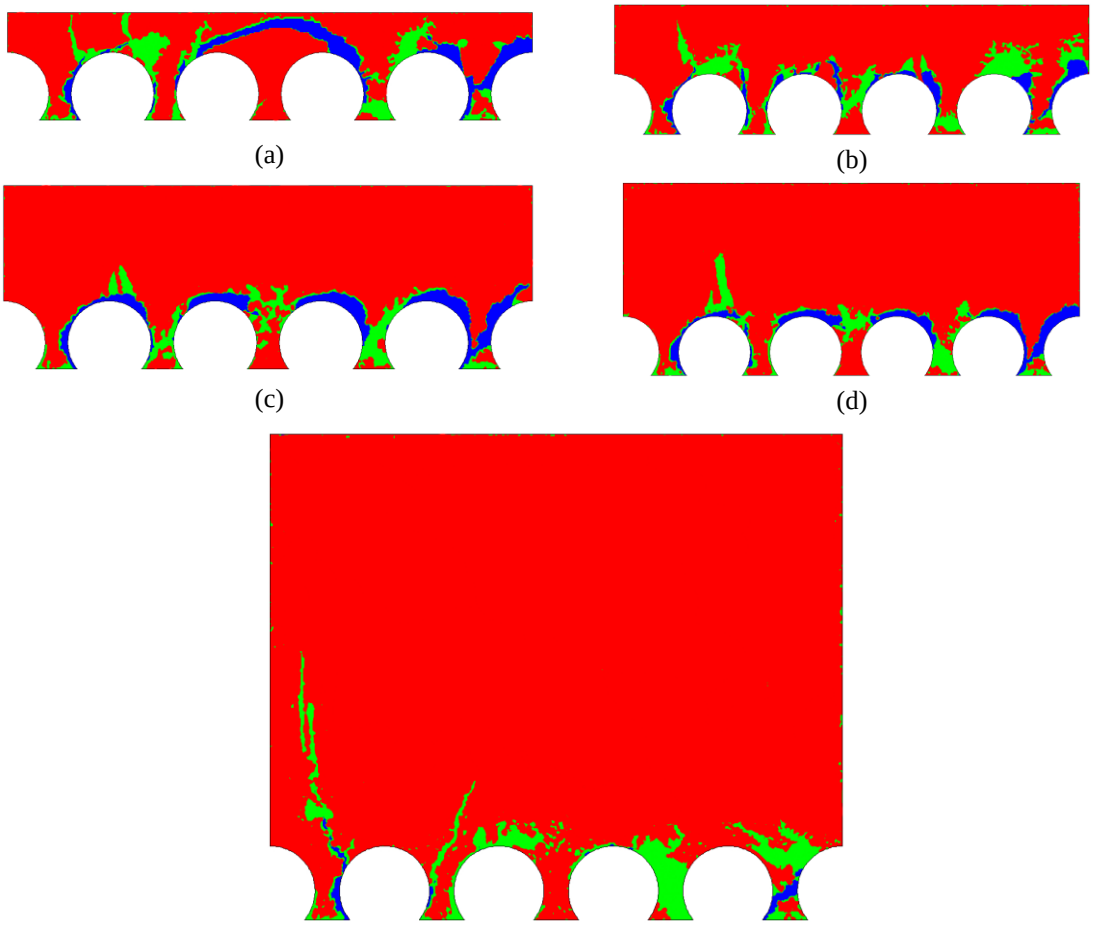

Fig. 6 Predicted tissue differentiation pattern after attainment of equilibrium for different size of polar gap with 20 μm normal, 20 μm tangential displacement: (a) 0.5 mm polar gap; (b) 1 mm polar gap; (c) 1.5 mm polar gap; (d) 2 mm polar gap; (e) 5 mm polar gap (Red: Bone; Green: Cartilage; Blue: Fibrous Tissue)

The present study, however, has a number of limitations. A 2-D plane strain model with bonded interface is a simplified representation of the original 3-D beaded geometry. A 3-D model of the beaded geometry with contact simulation at the interfaces would be more realistic representation of the implant-bone interface. However, the computational requirements for solving such problems would be far too larger. The assumption that MSC concentration will reach its maximum value at the end of sixteenth week may not be applicable for all patients. Moreover, clinical follow-up study and/or experimental measurements of cellular activity (migration and proliferation rates) with controlled displacements would be useful for validating the numerical results. However, this method is useful to predict tissue differentiation around any implant-bone interfaces having different beaded configurations on a comparative basis.

In the present study, implant-bone relative displacement was found to highly influence the peri-acetabular bone formation. During early post-operative period, for low implant-bone relative displacement of 20 μm, higher amount of cartilage formation (~55-70% of pore space) was

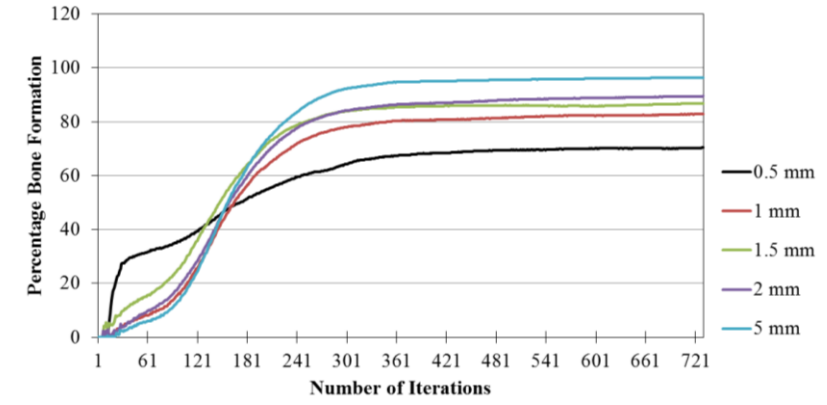

(a)

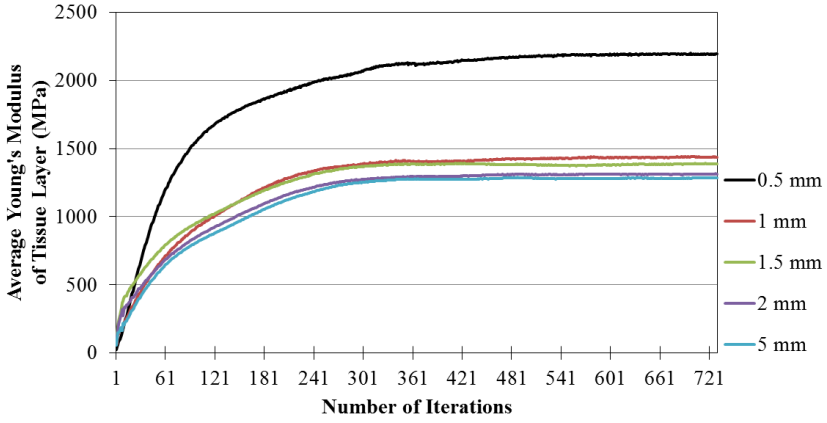

(b)

Fig. 7 Variation of tissue phenotypes and tissue Young's modulus with iterations for different size of polar gap: (a) Percentage of bone formed within the gap; (b) Average Young's modulus of the tissue layer

predicted within the gap, which was progressively transformed to bone. This observation is well supported by the study of Puthumanapully (2010), where similar trend of initial cartilage formation was observed for 2-layered and 3-layered Porocoat® beaded interface. After attainment of equilibrium for low implant-bone relative displacement, ~70% of pore space was filled with bone, which was higher than the bone ingrowth around porous Titanium acetabular shell (46%±20) (Hanzlik and Day 2013). However, the quantitative predictions of our study (~70%) were found to be more in agreement with the results of Bloebaum *et al.* (1997), which predicted 84%±9% bone ingrowth around Cancellous-Structured Titanium (CSTi). An increase in implant-bone relative displacement resulted in a reduction of bone growth and enhancement in fibrous tissue formation in the polar gap. At a higher relative displacement of 100 µm, a layer of fibrous tissue was observed to occupy ~60% of the polar gap. These trends are well supported with clinical results (Pilliar *et al.* 1986, Engh *et al.* 1993) and a few computational results employing tissue differentiation algorithm to predict bone ingrowth around multi-layered beads (Liu and Niebur 2008, Puthumanapully 2010). In general, all these studies predicted an increase fibrous tissue formation under high implant-bone micromotion, leading to a weak implant-bone interface.

The effect of acetabular polar gap on the extent of bone healing and peri-prosthetic bone ingrowth was found to be less pronounced. Polar gap upto 5 mm was found to progressively fill with bones under favourable implant-bone relative displacement. Similar observations were also predicted by several clinical studies (Sandborn *et al.* 1988, Schmalzried *et al.* 1994, Udomkiat *et al.* 2002, Springer *et al.* 2008, Takao *et al.* 2011, Nakasone *et al.* 2012) wherein, implant-bone gaps were progressively filled with newly formed bone. However, higher initial rate of bone formation was observed during low implant-bone gap of ~0.5 mm (similar to Sandborn *et al.* 1988). The change in average Young's modulus and the stiffness of the newly formed tissue layer in all the simulations (Fig. 7(b)) exhibited the characteristics S-shape (Richardson *et al.* 1994, Isaksson *et al.* 2006). Although bone healing was predominantly high within the polar gap, the average Young's modulus of the tissue layer decreased with an increase in the polar gap. This suggests the formation of low strength tissue for increased polar gap. Hence, a polar gap greater than ~0.5 mm seemed to weaken the implant-bone interface strength. Similar observations were also reported by Sandborn *et al.* (1988), wherein, a gap of 2 mm was reported as a critical gap in terms of limited rate of bone ingrowth.

5. Conclusions

The implementation of a mechano-regulatory tissue differentiation algorithm on 2D microscale plane strain FE models of implant bead-bone interface with polar gap have been useful in investigating the effects of implant-bone relative displacement and polar gap on peri-acetabular bone ingrowth. Based on the results of this study, it may be concluded that an increase in implant-bone relative displacement enhances fibrous tissue formation and reduces bone formation within the polar gap, thereby leading to weakening of the implant-bone interface strength. The effect of polar gap on bone healing and peri-acetabular bone ingrowth was less pronounced. However, the average Young's modulus of the newly formed tissue layer reduced with an increase in polar gap, suggesting the formation of low strength tissue for increased gap. It appears therefore, that a polar gap less than 0.5 mm seems favourable for increase in the strength of the implant-bone interface.

Acknowledgements

The authors would like to specially thank Dr. D. K. Nanda and Mr. A. Chattopadhyay of Computer and Informatics Centre, IIT Kharagpur for extending computational facilities required for the study.

References

Andreykiv, A., van Keulen, F. and Prendergast, P.J. (2008), "Simulation of fracture healing incorporating mechanoregulation of tissue differentiation and dispersal/proliferation of cells", *Biomech. Model Mechanobiol.*, **7**(6), 443-461.

Back, D.L., Dalziel, R., Young, D. and Shimmin, A. (2005), "Early results of primary Birmingham hip resurfacings: An independent prospective study of the first 230 hips", *J. Bone Joint Surg. Br.*, **87**(3), 324-329.

Bloebaum, R.D., Bachus, K.N., Jensen, J.W. and Hofmann, A.A. (1997), "Postmortem analysis of

consecutively retrieved asymmetric porous-coated tibial components", *J. Arthroplasty*, **12**(8), 920-929.
Bragdon, C., Jasty, M., Greene, M., Rubash, H.E. and Harris, W.H. (2004), "Biologic fixation of total hip implants: Insights gained from a series of canine studies", *J. Bone Joint Surg. Am.*, **86**, 105-117.
Carter, D.R., Blenman, P.R. and Beaupre, G.S. (1988), "Correlations between mechanical stress history and tissue differentiation in initial fracture healing", *J. Orthop. Res.*, **6**(5), 736-748.
Claes, L.E. and Heigele, C.A. (1999), "Magnitudes of local stress and strain along bony surfaces predict the course and type of fracture healing", *J. Biomech.*, **32**(3), 255-266.
Chou, H.Y. and Müftü, S. (2013), "Simulation of peri-implant bone healing due to immediate loading in dental implant treatments", *J. Biomech.*, **46**(14), 871-878.
Curtis, M.J., Jinnah, R.H. and Wilson, V.D. (1992), "The initial stability of uncemented acetabular components", *J. Bone Joint Surg. Br.*, **74**(3), 372-376.
Daniel, J., Pynsent, P.B. and McMinn, D.J.W. (2004), "Metal-on-metal resurfacing of the hip in patients under the age of 55 years with osteoarthritis." *J. Bone Joint Surg. Br.*, **86**(2), 177-184.
Davies, J.E. (1996), "In vitro modeling of the bone/implant interface", *Anat. Rec.*, **245**(2)**,** 426-445.
Davies, J.E. (2003), "Understanding peri-implant endosseous healing", *J. Dent. Edu.*, **67**(8), 932-949.
Dickinson, A., Taylor, A. and Browne, M. (2012), "Implant-bone interface healing and adaptation in resurfacing hip replacement", *Comp. Method. Biomech. Biomed. Engin.*, **15**(9), 935-947.
Engh, C.A., Bobyn, J.D. and Glassman, A.H. (1987), "Porous-coated Hip replacement: The factors governing bone ingrowth, stress shielding, and clinical results", *J. Bone Joint Surg. Br.*, **69**(1), 45-55.
Engh, C.A., Zettl-Schaffer, K.F., Kukita, Y., Sweet, D., Jasty, M. and Bragdon, C. (1993), "Histological and radiographic assessment of well functioning porous-coated acetabular components. A human postmortem retrieval study", *J. Bone Joint Surg. Am.*, **75**(6), 814-824.
Ghosh, R., Mukherjee, K. and Gupta, S. (2013), "Bone remodelling around uncemented metallic and ceramic acetabular components", *Proc. Inst. Mech. Eng. H.*, **227**(5)**,** 490-502**.**
Haddad, R.J., Cook, S.D. and Thomas, K.A. (1987), "Biological fixation of porous-coated implants", *J. Bone Joint Surg. Am.*, **69**(9)**,** 1459-1466.
Hanzlik, J.A. and Day, J.S. (2013), "Bone ingrowth in well-fixed retrieved porous tantalum implants", *J. Arthroplasty*, **28**, 922-927.
Hollister, S.J., Guldberg, R.E., Kuelske, C.L., Caldwell, N.J., Richards, M. and Goldstein, S.A. (1996), "Relative effects of wound healing and mechanical stimuls on early bone response to porous-coated implants", *J. Orthop. Res.*, **14**(4), 654-662.
Huiskes, R., van Driel, W.D., Prendergast, P.J. and Soballe, K. (1997), "A biomechanical regulatory model for periprosthetic fibrous tissue differentiation", *J. Mater. Sci. Mater. Med.*, **8**(12), 785-788.
Isaac, G.H., Siebel, T., Schmalzried, T.P., Cobb, A.G., O'Sullivan, T., Oakeshott, R.D., Flett, M. and Vail, T.P. (2006), "Development rationale for an articular surface replacement: a science-based evolution", *Proc. Inst. Mech. Eng. H.*, **220**(2), 253-268.
Isaksson, H., Wilson, W., van Donkelaar, C.C., Huiskes, R. and Ito, K. (2006), "Comparison of biophysical stimuli for mechanoregulation of tissue differentiation during fracture healing", *J. Biomech.*, **39**(8), 1507-1516.
Itayem, R., Arndt, A., Nistor, L., McMinn, D. and Lundberg, A. (2005), "Stability of the Birmingham hip resurfacing at two years:Aradiostereophotogrammetric analysis study", *J. Bone Joint Surg. Br.*, **87**(2), 158-162
Jasty, M., Bragdon, C.R., Maloney, W.J., Haire, T. and Harris, W.H. (1991), "Ingrowth of bone in failed fixation of porous-coated femoral components", *J. Bone Joint Surg. Am.*, **73**(9), 1331-1337.
Jasty, M., Bragdon, C.R., Burke, D., O'Connor, D., Lowenstein, J. and Harris, W.H. (1997), "In vivo skeletal responses to porous-surfaced implants subjected to small induced motions", *J. Bone Joint Surg. Am.*, **79**(5), 707-714.
Lacroix, D. and Prendergast, P.J. (2000), "A homogenization procedure to prevent numerical instabilities in poroelastic tissue differentiation models", *Proceedings of 8th Symposium on Computational Methods in Orthopaedic Biomechanics*, Orlando FL, March.
Lacroix, D. and Prendergast, P.J. (2002), "A mechano-regulation model for tissue differentiation during

fracture healing: analysis of gap size and loading", *J. Biomech.*, **35**(9), 1163-1171.
Lacroix. D., Prendergast, P.J., Li, G. and Marsh, D. (2002), "Biomechanical model to simulate tissue differentiation and bone regeneration: application to fracture healing", *Med. Biol. Eng. Comput.*, **40**(1), 14-21.
Liu, X. and Niebur, G.L. (2008), "Bone ingrowth into a porous coated implant predicted by a mechano-regulatory tissue differentiation algorithm", *Biomech. Model Mechanobiol.*, **7**(4), 335-344.
MacKenzie, J.R., Callaghan, J.J., Pedersen, D.R. and Brown, T.D. (1994), "Areas of contact and extent of gaps with implantation of oversized acetabular components in total hip arthroplasty", *Clin. Orthop. Relat. Res.*, **298**, 127-136.
Manley, M.T., Ong, K.L. and Kurtz, S.M. (2006), "The potential for bone loss in acetabular structures following THA", *Clin. Orthop. Relat. Res*, **453,** 246-253.
McMinn, D. and Daniel, J. (2006), "History and modern concepts in surface replacement", *Proc. Inst. Mech. Eng. H.*, **220**, 239-251.
Morrison, M.L. (2006), *Birmingham Hip Resurfacing System*, Materials and Processes for Medical Devices, October.
Nakasone, S., Takao, M., Nishii, T., Sakai, T. and Sugano, N. (2012), "Incidence and Natural Course of Initial Polar Gaps in Birmingham Hip Resurfacing Cups", *J. Arthroplasty*, **27**(9), 1676-1682.
National Joint Registry for England and Wales (2012), 9th Annual Report, Hemel, Hempstead, UK.
Peters, C.L. and Miller, M.D. (2006), *The Adult Hip*, Lippincott Williams and Wilkins, USA.
Pilliar, R.M., Lee, J.M. and Maniatopoulos, C. (1986), **"**Observations on the effect of movement on bone ingrowth into porous-surfaced implants", *Clin. Orthop. Relat. Res.*, **208**, 108-113.
Prendergast, P.J., Huiskes, R. and Søballe, K. (1997), "Biophysical stimuli on cells during tissue differentiation at implant interfaces", *J. Biomech.*, **30**(6), 539-548.
Puleo, D.A. and Nanci, A. (1999), "Understanding and controlling the bone-implant interface", *Biomater.*, **20**(23-24), 2311-2321.
Puthumanapully, P.K. (2010), "Simulation of tissue differentiation in uncemented hip implants based on a mechanoregulatory hypothesis", Ph.D. Dissertation, University of Southampton, Southampton.
Puthumanapully, P.K. and Browne, M. (2011), "Tissue differentiation around a short stemmed metaphyseal loading implant employing a modified mechanoregulatory algorithm: a finite element study", *J. Orthop. Res.*, **29**(5), 787-794.
Richardson, J.B., Cunningham, J.L., Goodship, A.E., O'Connor, B.T. and Kenwright, J. (1994), "Measuring stiffness can define healing of tibial fractures", *J. Bone Joint Surg. Br.*, **76**(3), 389-394.
Sandborn, P.M., Cook, S.D., Spires, W.P. and Kester, M.A. (1988), "Tissue response to porous-coated implants lacking initial bone apposition", *J. Arthroplasty*, **3**(4), 337-346.
Schmalzried, T.P., Wessinger, S.J., Hill, G.E. and Harris, W.H. (1994), "The Harris-Galante porous acetabular component press-fit without screw fixation, five-year radiographic analysis of primary cases", *J. Arthroplasty*, **9**(3), 235-242.
Slovakian Arthroplasty Register: Survival Analysis of Total Hip and Knee Replacement in Slovakia (2003-2011), Annual Report, Slovakia
Springer, B.D., Griffin, W.L., Fehring, T.K., Suarez, J., Odum, S. and Thompson, C. (2008), "Incomplete seating of press-fit porous-coated acetabular components: the fate of zone 2 lucencies", *J. Arthroplasty*, **23**(6), 121-126.
Takao, M., Nakamura, N., Ohzono, K., Sakai, T., Nishii, T. and Sugano, N. (2011), "The results of a press-fit-only technique for acetabular fixation in hip dysplasia", *J. Arthroplasty*, **26**(4), 562-568.
The New Zealand Joint Registry: Thirteen Year Report January 1999 to December 2011 (2012), New Zealand Orthopaedic Association, Wellington, New Zealand.
The Norwegian Arthroplasty Register (2010), Haukeland University Hospital, Haukeland, Norway.
Treacy, R.B.C., McBryde, C.W. and Pynsent, P.B. (2005), "Birmingham hip resurfacing arthroplasty: a minimum follow-up of five years", *J. Bone Joint Surg. Br.*, **87**(2), 167-170.
Treacy, R.B.C., McBryde, C.W., Shears, E. and Pynsent, P.B. (2011), "Birmingham hip resurfacing", *J. Bone Joint Surg. Br.*, **93**(1), 27-33.

Udomkiat, P., Dorr, L.D. and Wan, Z. (2002), "Cementless hemispheric porous-coated sockets implanted with press-fit technique without screws: average ten-year follow-up", *J. Bone Joint Surg. Am.*, **84**(7), 1195-1200.

US Food and Drug Administration (FDA) (2006), Birmingham Hip Resurfacing (BHR) System, online available at: http://www.accessdata.fda.gov/cdrh_docs/pdf4/P040033b.pdf.

ER